

The synergistic effect of 2,3,5,4'-Tetrahydroxystilbene-2-O- β -D-glucoside combined with Adriamycin on MCF-7 breast cancer cells

Jianfen Shen¹
Youzhi Zhang²
Hui Shen¹
Hua Pan¹
Longsheng Xu¹
Linna Yuan¹
Zhiying Ding¹

¹Department of Central Laboratory, The First Affiliated Hospital of Jiaxing University, Jiaxing 314000, China;

²School of Pharmacy, Hubei University of Science and Technology, Xianning 437100, China

Objective: Breast cancer has been reported to be a serious disease and a threat to women's health. 2,3,5,4'-Tetrahydroxystilbene-2-O- β -D-glucoside (THSG) is a bioactive natural compound originating from *Polygonum multiflorum* Thunb., which has been shown to possess anti-inflammatory and antitumor properties. Adriamycin (ADM) is a chemotherapy agent used in tumor therapy that is limited by its side effects. However, little is known about the synergistic effect of THSG combined with ADM on breast cancer. This study seeks to investigate the effects of the combination of THSG plus ADM on MCF-7 breast cancer cells and to test the mechanisms involved.

Materials and methods: MTT assay was detected to determine cell viability. Furthermore, cell apoptosis was tested by flow cytometry and TUNEL assay. In addition, protein expression was measured by Western blot analysis.

Results: The individual treatment of THSG and ADM induced cell injury. Moreover, cotreatment further increased it, which the effect may be associated with the elevation of the apoptotic-related protein expression such as Bax/Bcl-2 and cleaved caspase-3/caspase-3. Lastly, our results also show the reduction of vascular endothelial growth factor/phosphatidylinositol 3-kinase/Akt protein expression in the individual or synergistic treatment.

Conclusion: Taken together, cotreatment of THSG and ADM may exert a synergistic reduction of cell injury via the inhibition of vascular endothelial growth factor/phosphatidylinositol 3-kinase/Akt pathway. Thus, THSG might possess potent anti-breast cancer effect with ADM.

Keywords: THSG, ADM, synergistic effect, apoptosis, VEGF/PI3K/Akt, breast cancer

Introduction

Breast cancer occurs in approximately 12% of women, but it accounts for 14% of all cancer-related deaths worldwide.¹ Over 70% of breast cancer cases are positive for estrogen receptor (ER), which is the most common subtype of breast cancer among women.² In addition, nearly 1.2 million new ER-positive breast cancer cases were diagnosed in 2012 worldwide (<http://www.wcrf.org>). Relevant to this study, chemotherapy continues to be recommended as the standard treatment for most ER-positive breast cancers, but its use is limited by systematic adverse effects and multidrug resistance resulting in low sensitivity. Adriamycin (ADM) is a chemotherapy agent used in the adjuvant and neoadjuvant settings in breast cancer.³ However, it is limited due to a severe cardiotoxic side effect that manifests in a dose-related manner.⁴ The mechanisms underlying the effects on cardiac tissue, such as DNA damage, free radical formation, lipid peroxidation, and activation

Correspondence: Youzhi Zhang
School of Pharmacy, Hubei University of Science and Technology, No. 88, Xianning Avenue, Xianning 437100, China
Tel +86 715 827 2135
Email yzhang242@hbust.edu.cn

of proapoptotic signaling cascades, were all intensively investigated.⁵ To reduce the adverse reactions while maintaining antitumor effects, the classic strategy was to develop combination therapies, including pairings with antibodies, peptides, synthetic polymers, or natural products.⁶

2,3,5,4'-Tetrahydroxystilbene-2-O- β -D-glucoside (THSG) is an active compound derived from *Polygonum multiflorum* Thunb. that shows better water solubility than its structural analog resveratrol, which belongs to the hydroxystilbene compound family. Resveratrol and its analogs show antitumor effects in breast cancer.⁷ THSG suppressed human colorectal cancer cell metastasis⁸ and adhesion and invasion of human lung cancer cells,^{9,10} indicating an antitumor effect. THSG inhibited vascular endothelial growth factor (VEGF) protein expression in foam cells.¹¹ Additionally, studies demonstrated that THSG could protect against ADM-induced cardiotoxicity by suppressing the apoptotic signaling pathway¹² and against ADM-induced nephropathy by activating the Nrf2-Keap1 antioxidant pathway.¹³ Accordingly, these studies indicated that THSG may serve as an effective complementary agent in the treatment of MCF-7 breast cells.

In this study, we hypothesized that THSG possessed the antitumor property of suppressing cell proliferation, investigated the synergistic effect of THSG in combination with ADM on MCF-7 cells (an ER-positive breast cancer cell line), and evaluated the synergistic effects of the applied agents through the Chou-Talalay assay. The underlying mechanisms of the combination therapy were investigated as well. Taken together, the results show that THSG could be a novel agent in the anti-breast cancer drug formulary, and the combination of THSG with ADM may be a novel strategy for the amelioration of side effects and multidrug resistance to antitumor drugs.

Materials and methods

Cell lines, culture conditions, and reagents

MCF-7 is an ER-positive human breast cancer cell line, and H1299 (human lung cancer cell line) and LNC (prostate cancer cell line) were supplied by the Cell Bank of the Chinese Academy of Sciences (Shanghai, China) and cultured in DMEM (Gibco, Waltham, MA, USA), supplemented with 10% FBS (Gibco) in a humidified incubator at 37°C and 5% CO₂. THSG was purchased from Chengdu Herbpurify Co., Ltd. (NO: E-022-160001, Chengdu, China) and prepared as a 10 mM stock solution in a medium supplemented with 2% FBS. ADM was purchased from the National Standard Material Sales Center (Beijing, China) and prepared as a 10 mM stock solution in normal saline, which

was serially diluted in medium supplemented with 2% FBS immediately prior to experiments. DMEM, FBS, penicillin, and streptomycin were purchased from Gibco. All other reagents were of analytical grade.

Cell viability assay

Cell viability was evaluated with an MTT assay according to the manufacturer's instructions. Briefly, MCF-7, H1299, and LNC cells (10 \times 10³/well) were plated into 96-well plates in triplicate and cultured for 24 hours before treatment. Then, the cells were treated with THSG and ADM for 24 or 48 hours over a wide dose range to make growth curves, which were used as guides to decide on a fixed molar ratio and to identify the concentrations of both drugs in combination. Cells were incubated with MTT (0.5 mg/mL) at 37°C for 4 hours and then treated with 100 μ L/well dimethyl sulfoxide after the removal of the medium. The absorbance values were determined at a wavelength of 570 nm with a 630 nm reference using a microplate reader (BioTek Instruments, Winooski, VT, USA). Cell viability was calculated from the optical density (OD) with the following formula: cell viability (%) = (OD value of treatment group/OD value of control group). The IC₅₀ (50% inhibitory concentration) value was calculated by nonlinear regression analysis with GraphPad Prism software.

Synergy determination

The Chou-Talalay method was applied to determine the combination index (CI) in the analysis of the combination study. The data obtained from the MTT assay were used to calculate the proliferative inhibition rate (%) with the following formula: (1-treatment group/control group). Then, the data were transformed to fraction affected (Fa; the range 0–1), where Fa = 0 and 1 represented 100% viability and 0% viability, respectively, and input into CompuSyn software (Biosoft, Ferguson, MO, USA); the data were also used to calculate the dose ratios on the basis of the Chou and Talalay median-effect principle.^{14,15} The effects of the combinations of the two drugs were primarily reflected by the CI values, where CI < 1 demonstrates synergism, CI = 1 indicates an additive effect, and CI > 1 indicates antagonism.¹⁶

Analysis of cell apoptosis by TUNEL assay

MCF-7 cell apoptosis was determined with an In Situ Cell Death Detection Kit (Roche, Merck KGaA, Darmstadt, Germany). According to the manufacturer's protocol, cells were fixed with 4% paraformaldehyde for 1 hour. Terminal deoxynucleotidyl transferase solution was dissolved in the dark, added to the cells, and incubated for 60 minutes at 37°C.

Then, the cells were washed twice in PBS buffer for 5 minutes each time. TUNEL-positive cells (green) that were also dyed with DAPI (blue) were identified as apoptotic cells under a fluorescence microscope. The percentage of apoptotic cells was determined by counting the TUNEL-positive cells and dividing the number by the total number of cells.

Analysis of cell apoptosis by flow cytometry

MCF-7 cell apoptosis was also measured using an Annexin V-FITC Apoptosis Detection Kit (Cat. 11684795910, Roche) according to the manufacturer's protocol. Briefly, the MCF-7 cells were trypsinized and then harvested by centrifugation at $200\times g$ at 4°C for 15 minutes. The cells were suspended in a staining buffer containing anti-Annexin V-FITC antibody and propidium iodide (PI) at room temperature for 15 minutes. The stained samples were then analyzed using flow cytometry (BD LSRFortessa™; BD Biosciences, San Jose, CA, USA), and the percentage of apoptotic cells was determined from the Annexin V/PI ratio. The Annexin V staining intensity was set as the horizontal axis, and the PI staining intensity was set as the vertical axis.

Western blot analysis

Western blot analysis was performed as described previously.¹⁷ In brief, proteins from the MCF-7 cells were extracted using a sucrose buffer (20 mM HEPES, 1 mM EDTA, 255 mM sucrose, and a cocktail of protease inhibitors; pH 7.4). After boiling for 5 minutes at 95°C in a $2\times$ loading buffer, 50 μg total protein were loaded and separated by 10% or 15% SDS-PAGE. The proteins were then electrophoretically transferred at 100 V for 1 hour into a PVDF membrane (EMD Millipore, Billerica, MA, USA). The membrane was blocked with 4% nonfat milk in Tris-buffered saline containing Tween 20. After washing, the membrane was probed with a 1:1,000 dilution of primary mouse or rabbit antibody against Bax (32503, Abcam), Bcl-2 (32124, Abcam), caspase-3 (32351, Abcam), cleaved caspase-3 (32042, Abcam), VEGF (MAB293-100, R&D), p-Akt (131443, Abcam), p-phosphatidylinositol 3-kinase (PI3K; 13857s, Cell Signaling), or GAPDH (8245, Abcam) overnight at 4°C followed by incubation with a second antibody (Abcam 6721, goat antirabbit or Abcam 6789, goat antimouse). The immunoreactive bands were detected using a Syngene instrument (Syngene, Bangalore, India). Densitometry analysis of the images was performed using GeneTools from Syngene Software.

Statistical analyses

Data are presented as mean \pm standard error of the mean (SEM). Significant differences between and within multiple

groups were examined using one-way ANOVA followed by Bonferroni's multiple range test. Statistical analysis was performed with GraphPad Prism software. $P < 0.05$ was considered statistically significant.

Results

Cotreatment with THSG and ADM synergistically suppressed the cell viability of MCF-7 cells

As shown in Figure 1A, THSG and ADM decreased cell viability, with a higher IC_{50} value (359.6 μM) for THSG and a lower IC_{50} value (0.78 μM) for ADM in MCF-7 cells at 48 hours. These data demonstrated that MCF-7 cells possessed a stronger sensitivity to ADM than THSG. However, IC_{50} value is 620.6 μM and 471.3 μM at the treatment of THSG in H1299 and LNC cells, respectively (Figure 1D and E). The data suggested that MCF-7 cells possessed a stronger sensitivity compared with H1299 and LNC cells. Furthermore, we also detected the effect of individuals or combination at 24 hours in Figure 2A, in which IC_{50} value is 685.6 μM and 2.19 μM at the treatment of THSG and ADM, respectively.

Given the IC_{50} value determined for the individual drugs, the drug combination of THSG and ADM was administered at 400:1 (THSG:ADM) fixed molar ratio for 48 hours and showed an IC_{50} value of $164.6 + 0.41 \mu\text{M}$. The drug combination treatment was given as effect-oriented and exerted a synergistic inhibitory effect ($\text{CI} < 1$) with an Fa value ≥ 0.45 from the Fa-CI plot (Figure 1B). As shown in Figure 1C, the drug combination value was given as dose oriented from the isobologram at Fa = 0.5, 0.75, and 0.9. These data are summarized for concise formation at Fa = 0.9 in Table 1. The data suggested that the drug combination resulted in a much stronger inhibition than either individual treatment. However, as shown in Figure 2B and C, the drug combination treatment was given as effect-oriented and exerted an antagonism ($\text{CI} > 1$) from the Fa-CI plot at 24 hours. Furthermore, treatment with 200 μM THSG and 0.5 μM ADM for 48 hours was performed in the next experiments based on the cell IC_{50} value, which was regulated moderately.

Cotreatment with THSG and ADM synergistically induced cell apoptosis

Then, we examined cell apoptosis by flow cytometry and TUNEL assay at 48 hours. As shown in Figure 3A and C, THSG primarily increased the proportion of cells in early apoptosis (33.8 ± 7.19 , dots in Q4). However, ADM increased the

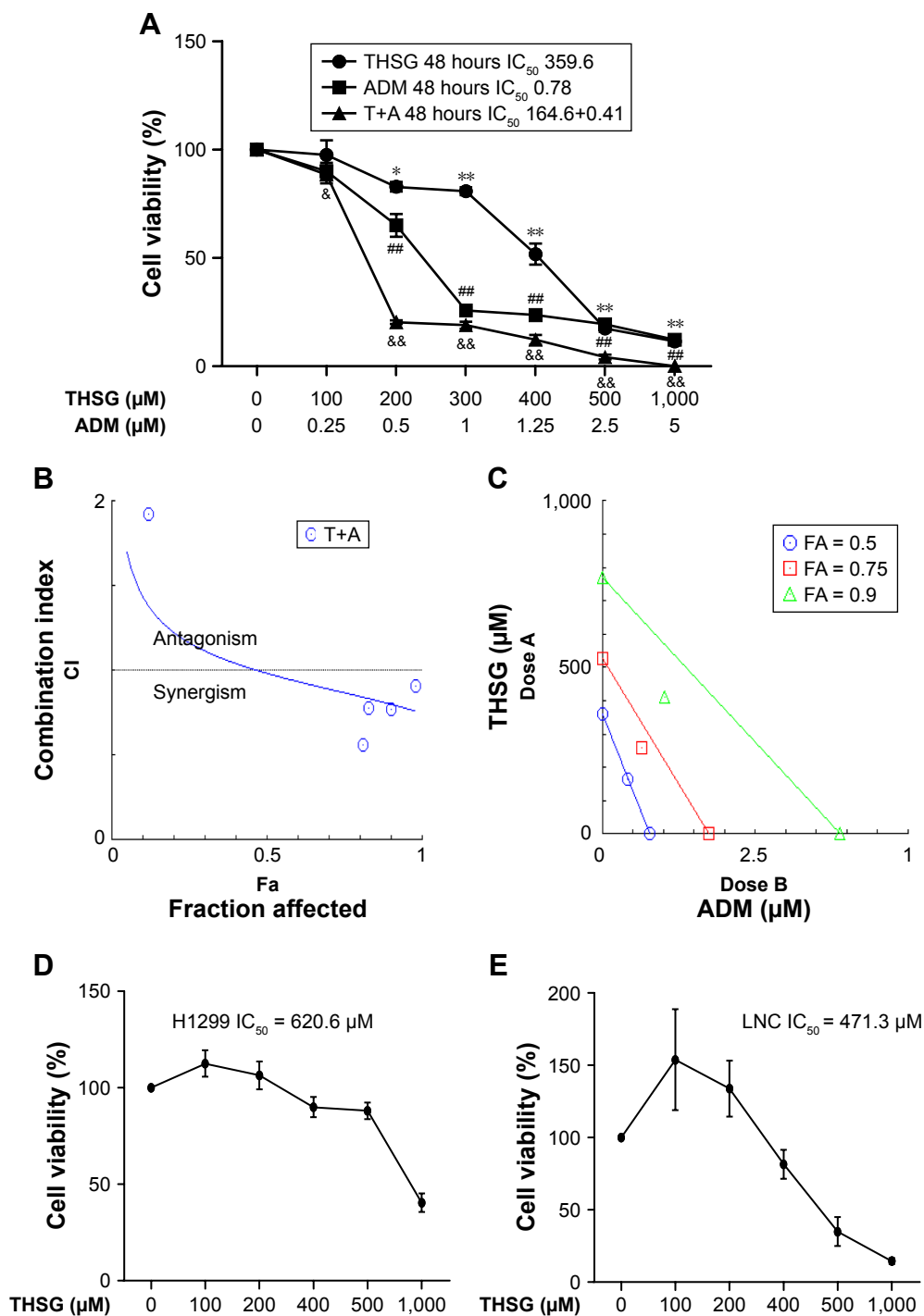


Figure 1 The proliferative inhibition assay of THSG, ADM, and THSG in combination with ADM on different cell lines.

Notes: Cells were exposed to various concentrations of THSG and ADM alone or in combination at 400:1 molar ratio for 48 hours. **(A)** Cell viability curves were plotted based on the MTT assay in MCF-7 cell lines. The synergistic effects between drugs were shown as CI-Fa plot **(B)**; isobologram **(C)** was calculated with the Calcsyn™ software. **(B)** CI values are represented by points above (indicate antagonism) or below the lines (indicate synergism). **(C)** Isobologram analysis represents the individual doses of drugs in the achievement of 90% growth inhibition ($\text{Fa} = 0.9$), 75% growth inhibition ($\text{Fa} = 0.75$), and 50% growth inhibition ($\text{Fa} = 0.5$). **(D)** Cell viability of THSG was performed based on the MTT assay in H1299 cell lines. **(E)** Cell viability of THSG was performed based on the MTT assay in LNC cell lines. * $P < 0.05$, ** $P < 0.01$ vs the Ctr group with THSG; ### $P < 0.01$ vs the Ctr group with ADM; & $P < 0.05$, && $P < 0.01$ vs the Ctr group with THSG.

Abbreviations: ADM, Adriamycin; CI, combination index; Ctr, control; T+A, THSG + Adriamycin; THSG, 2,3,5,4'-Tetrahydroxystilbene-2-O- β -D-glucoside.

proportion of cells in both early (dots in Q4) and late apoptosis (dots in Q2), but this increase was not significant. Although the drug combination elevated the proportion of cells in both early and late apoptosis, only the increase in late apoptosis

(dots in Q2) was significant, as shown in Figure 3A–C. Given that the individual and the combination treatments varied in the significance of the increases in early apoptosis and late apoptosis, we further examined early plus late apoptosis,

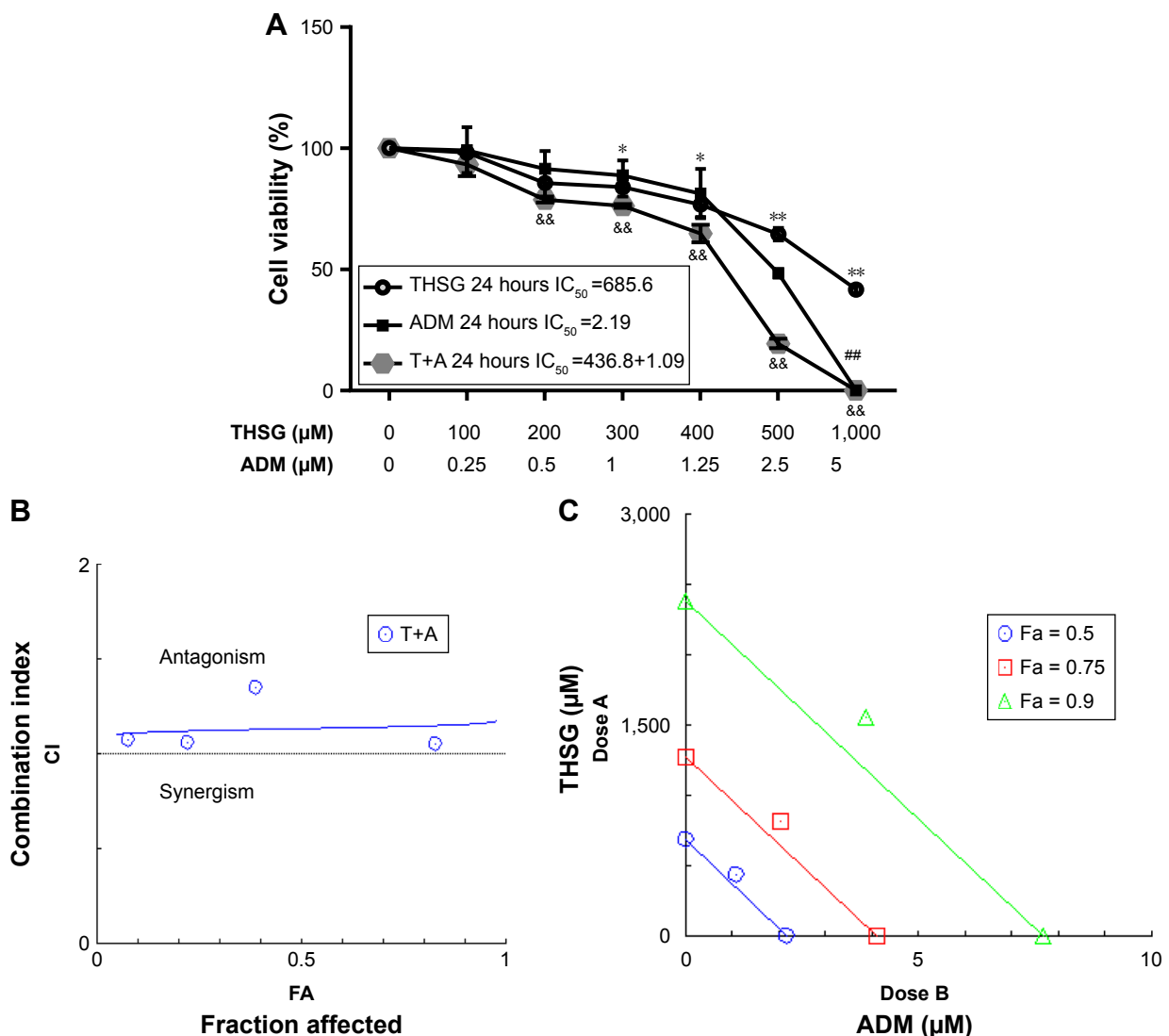


Figure 2 The proliferative inhibition assay of THSG, ADM, and THSG in combination with ADM on MCF-7 cell lines.

Notes: Cells were exposed to various concentrations of THSG and ADM alone or in combination at 400:1 molar ratio for 24 hours. **(A)** Cell viability curves were plotted based on the MTT assay in MCF-7 cell lines. The antagonism effects between drugs were shown as CI-Fa plot **(B)**, isobologram **(C)** calculated with the Calcsyn™ software. **(B)** CI values are represented by points above (indicate antagonism) or below the lines (indicate synergism). **(C)** Isobologram analysis represents the individual doses of drugs in the achievement of 90% growth inhibition (Fa = 0.9), 75% growth inhibition (Fa = 0.75), and 50% growth inhibition (Fa = 0.5). * $P < 0.05$, ** $P < 0.01$ vs the Ctr group with THSG; ### $P < 0.01$ vs the Ctr group with ADM; ** $P < 0.01$ vs the Ctr group with THSG.

Abbreviations: ADM, Adriamycin; Ctr, control; T+A, THSG + Adriamycin; THSG, 2,3,5,4'-Tetrahydroxystilbene-2-O- β -D-glucoside.

which were markedly significant for the individual and the combination treatments (Figure 3D). In addition, a TUNEL assay was performed to detect DNA fragmentation, which confirmed the results from flow cytometry. As shown in Figure 3E and F, individual treatment and cotreatment groups showed more cell apoptosis, as shown by TUNEL staining

(stained green cells) compared with the control group in MCF-7 cells. However, we detected cell apoptosis with the combination treatments at 24 hours in Figure 4A–D, which showed that the apoptotic rate is only 26.7% (Q2+Q4) when treated with T+A. Furthermore, similarities in cell morphology and growth status were also investigated under an inverted phase microscope in Figure 3G.

Table I The concise formation of combination drug at Fa = 0.9

Drug	CI value	Dose T (μM)	Dose A (μM)
THSG		770.522	
ADM			3.89251
T+A	0.80124	412.995	1.03249

Abbreviations: ADM, Adriamycin; CI, combination index; T+A, THSG + Adriamycin; THSG, 2,3,5,4'-Tetrahydroxystilbene-2-O- β -D-glucoside.

Cotreatment with THSG and ADM synergistically regulated protein activity

Next, we determined whether the combination of drugs regulated apoptosis-related proteins in MCF-7 cells. As shown in Figure 5A and B, individual treatment with THSG

or ADM increased Bax protein expression but reduced Bcl-2 expression, but the change was not statistically significant. A similar effect was found with the combination treatment. We further determined that the combination markedly elevated the ratio of Bax/Bcl-2, but individual drug treatment

did not significantly affect the ratio. Such elevations in apoptosis-related protein expression were further confirmed by enhanced processing of caspase-3 to its bioactive form, cleaved caspase-3. As shown in Figure 5C and D, individual treatment and combination treatment promoted an increase in

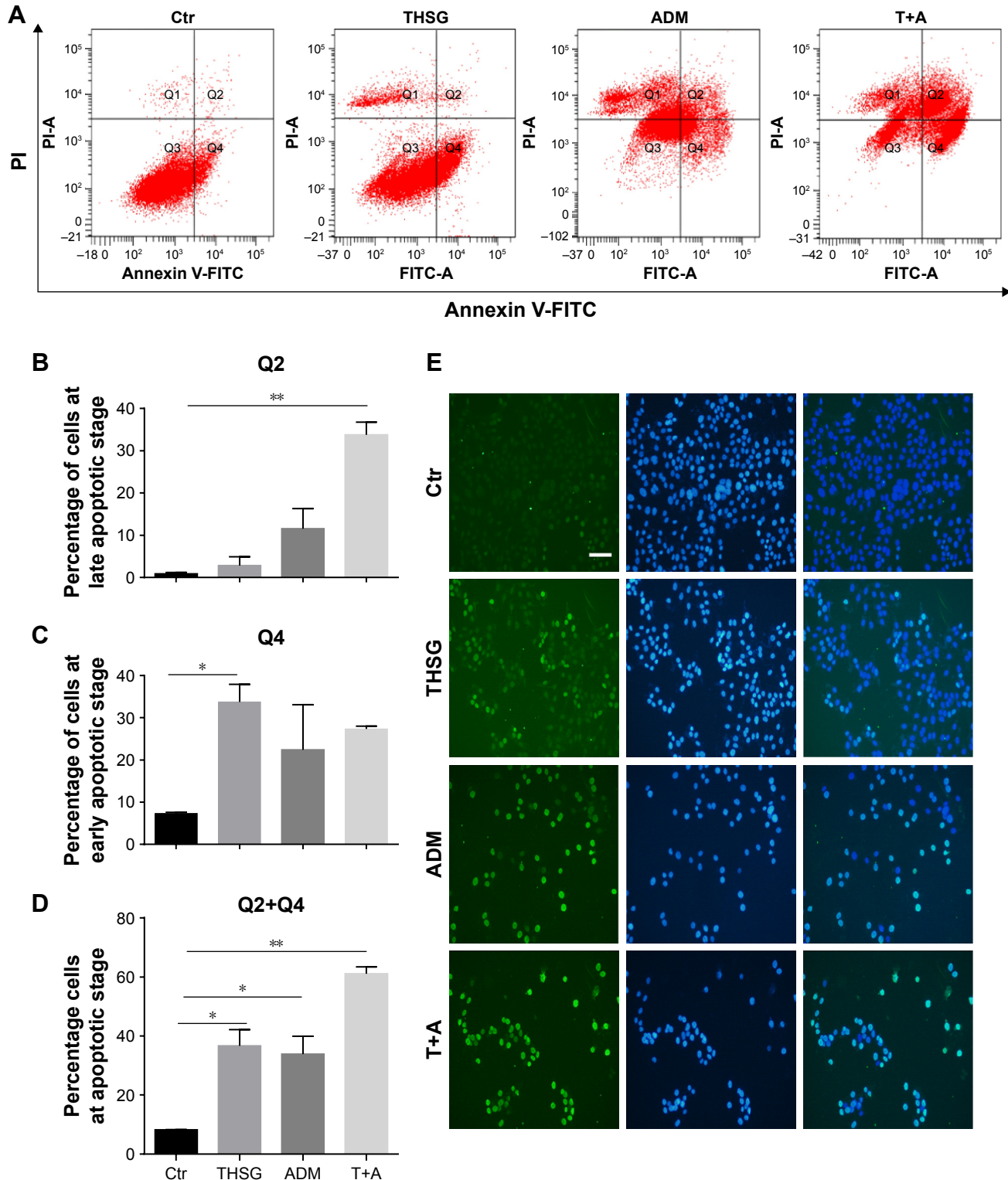


Figure 3 (Continued)

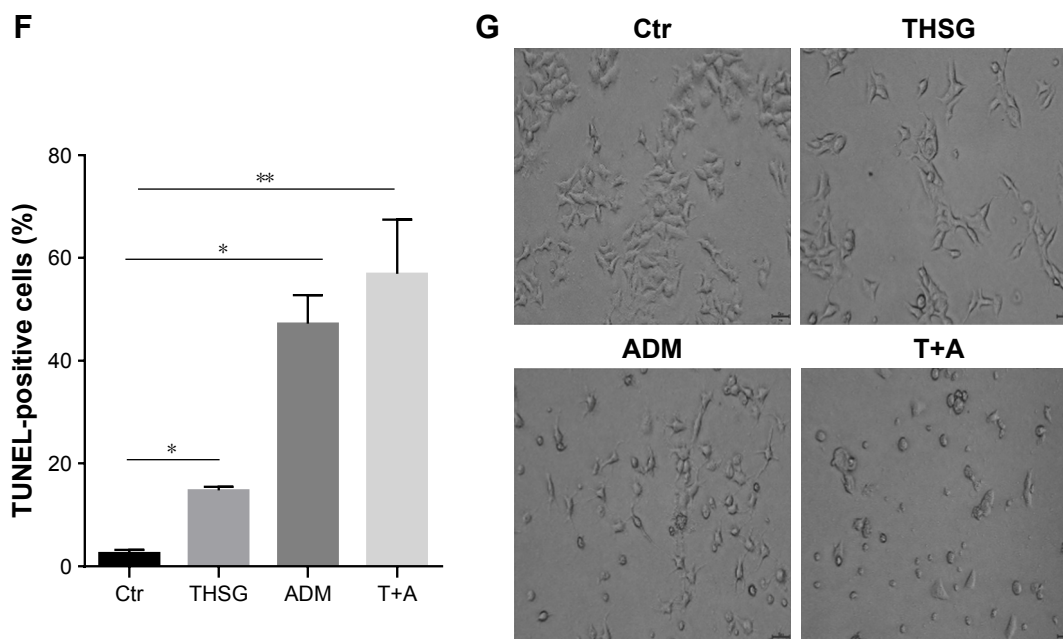


Figure 3 Effect of THSG and ADM individual and in combination on the apoptosis in MCF-7 cells.

Notes: (A) The apoptosis rate after 48-hour treatment with 200 μ M of THSG and 0.5 μ M of ADM individual or in combination with flow cytometry. (B) Representative graph of late apoptosis (Q2 dots). (C) Representative graph of early apoptosis (Q4 dots). (D) Representative graph of late + early apoptosis (Q2+Q4 dots). (E) Representative photographs of TUNEL staining cells (green) and DAPI-positive cells (blue) in various groups. (F) Histogram of quantification of TUNEL was shown with the percentage of TUNEL-positive nuclei (green) relative to DAPI-positive total nuclei (blue). (G) Morphology and growth status under an inverted phase microscope. All data represent mean \pm SEM of three independent experiments. Bars = 50 μ m. * P <0.05, ** P <0.01 vs the Ctrl group.

Abbreviations: ADM, Adriamycin; Ctr, control; PI, propidium iodide; T+A, THSG + Adriamycin; THSG, 2,3,5,4'-Tetrahydroxystilbene-2-O- β -D-glucoside.

the ratio of cleaved caspase-3/caspase-3. Additionally, VEGF and the PI3K/Akt pathway affect cell survival and apoptosis in human breast cancer. As shown in Figure 5E and F, both individual and combination treatments reduced VEGF expression. Similar results were found for p-PI3K and p-Akt protein expression.

Discussion

In this study, we illustrated that the combined treatment of THSG and ADM could inhibit cell viability, induce apoptosis, and suppress cell migration in MCF-7 breast cancer cells in a synergistic manner. Additionally, our results indicated that the underlying mechanism of the combination treatment may be associated with the suppression of the VEGF/PI3K/Akt pathway.

In our study, THSG exerted an inhibitory effect on cell viability in MCF-7 cells, which was in accordance with the following report that the sensitivity to THSG varies in different types of cancer cells; THSG inhibited cell viability in A549 lung cancer cells⁹ or prevented HT-29 colorectal cancer cell metastasis⁸ and inhibited B16F1 melanoma cell proliferation.¹⁸ Notably, most studies supported the observation that THSG exhibited suppression in a variety of cancer cells. Although MCF-7 cells were more sensitive to ADM than THSG according to the IC_{50} values shown

in Figure 1, the clinical uses of ADM are limited due to severe adverse reactions. Thus, drug combination is one of the main strategies for ADM use. Cumulative data have demonstrated that ADM-induced cardiotoxicity is reduced by some natural products, such as Tanshinone IIA,¹⁹ flavaglin,²⁰ and resveratrol,²¹ through various types of mechanisms in cells and animal models. THSG is a resveratrol analog with an additional glycoside moiety that increases the hydrophilicity of aglycone and promotes excretion in the urine.¹⁰ Cumulative data have demonstrated that resveratrol abolishes doxorubicin resistance in breast cancer cells and strengthens doxorubicin-induced chemosensitivity.^{22,23} Additionally, a small number of studies have indicated that THSG exhibits a protective effect against doxorubicin-induced cardiotoxicity.¹² In this study, for the first time, the synergistic effect of THSG and ADM in MCF-7 breast cancer cells was demonstrated through a Chou-Talalay assay in which the combination reduced the required ADM concentration and avoided higher dose of ADM associated with cell toxicity in normal cardiac cells.²² In contrast, the study showed almost no synergistic effect in MCF-7 cells at the THSG doses used in combination of doxorubicin and THSG study,²⁴ which may be due to the purity produced by the manufacturers. Notably, the concentration of THSG required for synergism has been reported to have no toxicity in normal cardiac cells.¹² Accordingly, THSG in combination

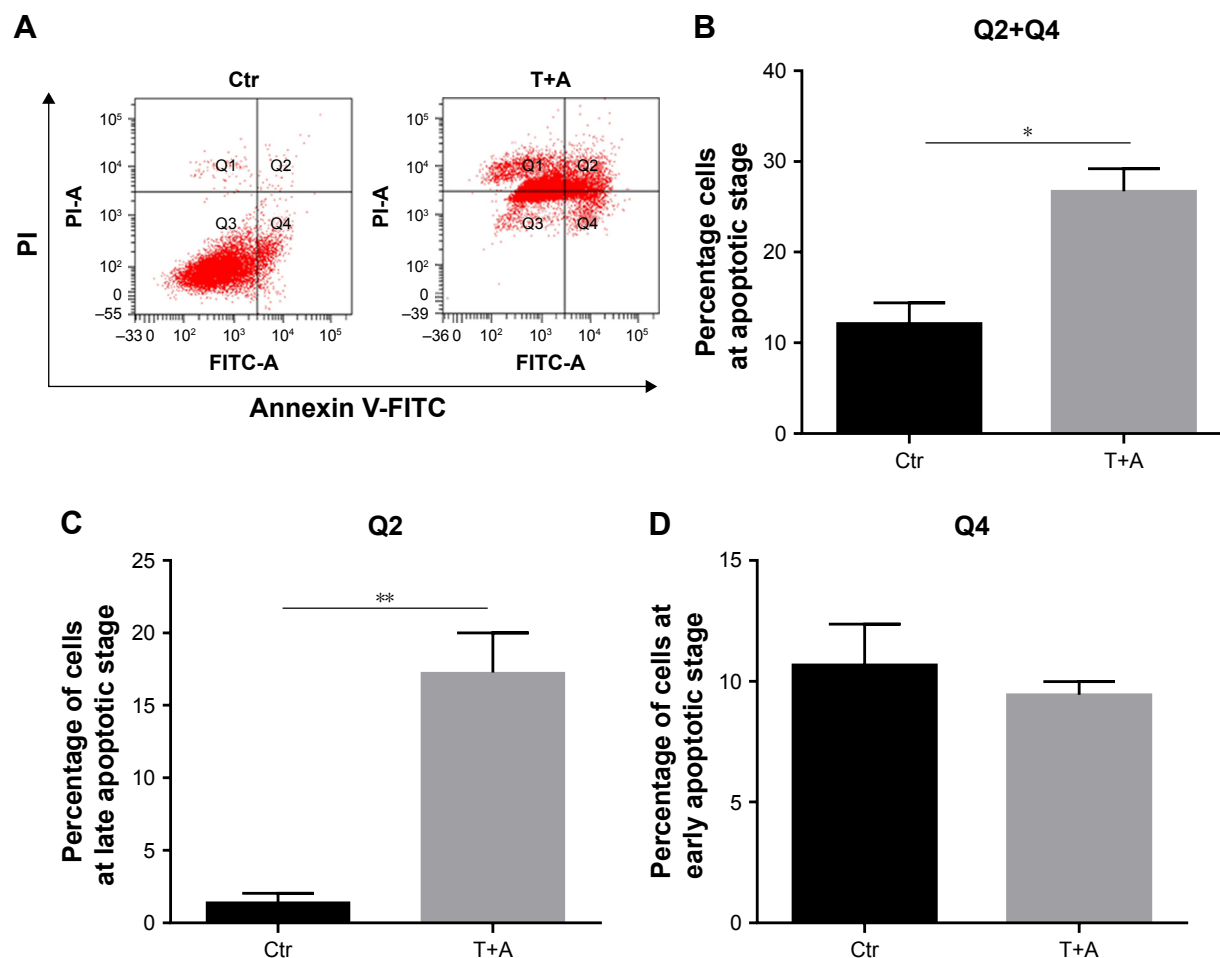


Figure 4 Effect of THSG and ADM in combination on the apoptosis in MCF-7 cells.

Notes: (A) The apoptosis rate after 24-hour treatment with 200 μM of THSG and 0.5 μM of ADM in combination with flow cytometry. (B) Representative graph of late + early apoptosis (Q2+Q4 dots). (C) Representative graph of late apoptosis (Q2 dots). (D) Representative graph of early apoptosis (Q4 dots). All data represent mean \pm SEM of three independent experiments. Bars = 50 μm . * $P < 0.05$, ** $P < 0.01$ vs the Ctr group.

Abbreviations: ADM, Adriamycin; Ctr, control; PI, propidium iodide; T+A, THSG + Adriamycin; THSG, 2,3,5,4'-Tetrahydroxystilbene-2-O- β -D-glucoside.

with ADM not only reduced the ADM dose to levels below the dose that causes side effects but also safely treated MCF-7 cells as an individual therapy.

Our observations revealed that the inhibition of cell viability by individual treatment or combination treatment may be associated with the suppression of VEGF. VEGF is a master gene promoting tumor angiogenesis. Earlier studies proved that a water-soluble fraction of *P. multiflorum* Thunb. suppressed the expression of VEGF and intercellular adhesion molecule-1 in foam cells,¹¹ and THSG could inhibit lysophosphatidylcholine-induced expression of VEGF in the human umbilical vein endothelial cell line.²⁵ However, a study showed a different effect of THSG on VEGF expression, where it significantly upregulated VEGF expression and promoted angiogenesis in ischemia/reperfusion-induced brain injury in rats.²⁶ The reason for the discrepancy between these studies is unknown and may be due to the sources or types of tissue,

as the opposite effects were observed between brain injury and cancer cells. In this study, the individual treatment and combination treatment inhibited VEGF protein expression. Nonetheless, these studies support the notion that THSG could affect VEGF expression in various types of tissue, and the underlying mechanism needs to be further explored.

PI3K/Akt signaling is downstream of the VEGF pathway in breast tumor progression.²⁷ Hyperactivation of the PI3K/Akt pathway is associated with tumorigenesis, cancer progression, and drug resistance in almost all human cancers.^{28,29} Currently, preclinical data on the inhibition of this pathway were supportive, and Phase I–III trials using inhibitors of the pathway have been conducted in breast cancer.³⁰ Consistent with these previous studies, the present findings demonstrated that individual treatment with THSG or ADM could reduce PI3K/Akt protein expression. A similar inhibitory effect was found with the treatment of the combination of drugs. PI3K is

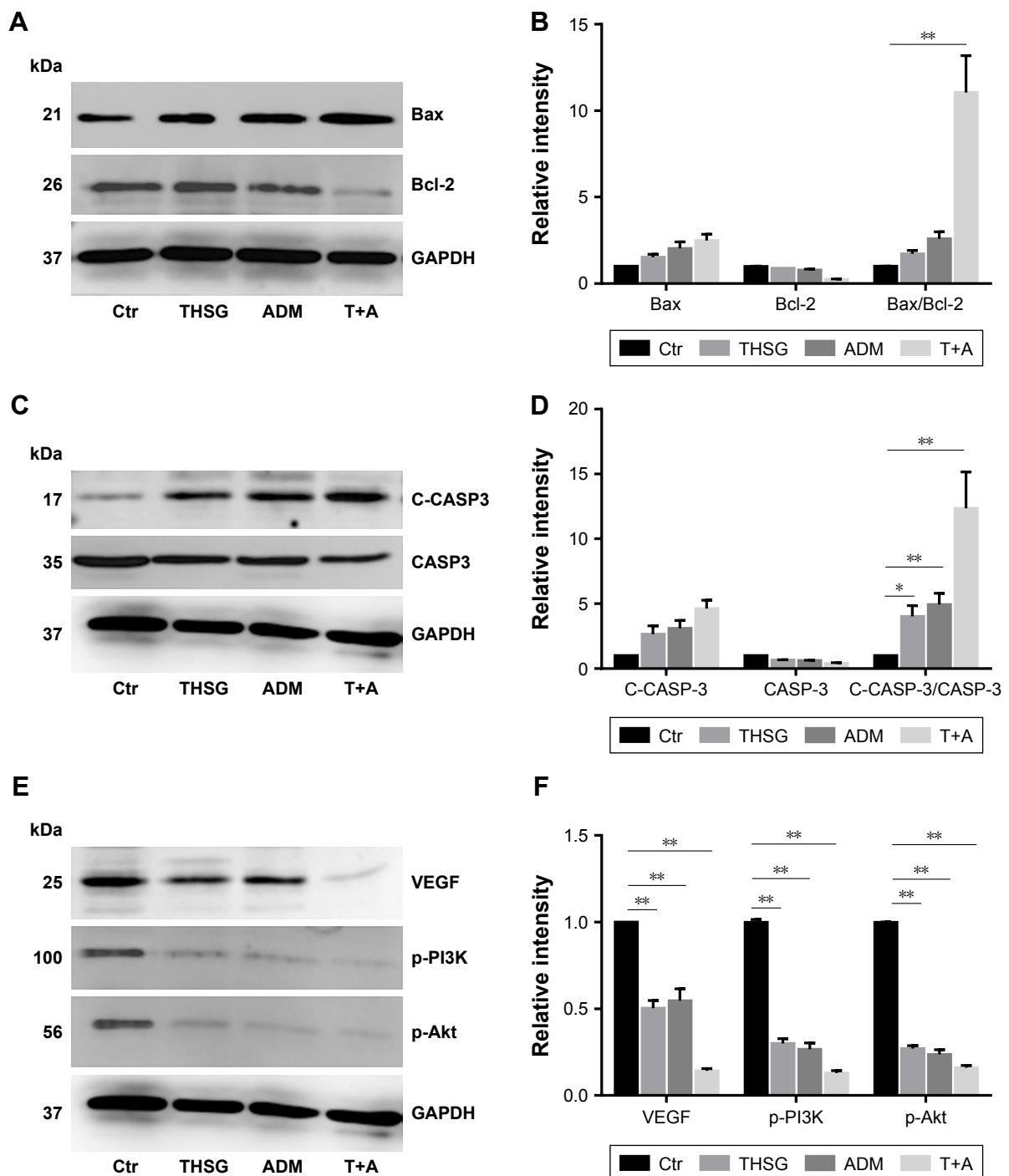


Figure 5 Effects of THSG and ADM on the inhibition of VEGF/PI3K/Akt signaling pathway in MCF-7 cells.

Notes: The expression levels of various proteins with 200 μ M of THSG and 0.5 μ M of ADM individual or in combination for 48 hours. **(A)** Representative protein band of Bax and Bcl-2. **(B)** Representative optical density of the tests protein Bax, Bcl-2, and Bax/Bcl-2. **(C)** Representative protein band of caspase-3 and cleaved caspase-3. **(D)** Representative optical density of caspase-3, cleaved caspase-3, and cleaved caspase-3/caspase-3. **(E)** Representative protein band of VEGF, p-PI3K, and p-Akt. **(F)** Representative optical density of VEGF, p-PI3K, and p-Akt. Data are presented as mean \pm SEM of three independent experiments. * P <0.05, ** P <0.01 vs the Ctr group. **Abbreviations:** ADM, Adriamycin; CASP3, caspase-3; C-CASP3, cleaved caspase-3; Ctr, control; T+A, THSG + Adriamycin; THSG, 2,3,5,4'-Tetrahydroxystilbene-2-O- β -D-glucoside.

activated by VEGF binding to its receptors, which is known to induce angiogenesis.³¹ Thus, the inhibition of cell proliferation and the synergism of the drugs were presumably associated with inhibition of VEGF and downstream pathways

of PI3K/Akt protein expression. The PI3K/Akt pathway modulates many cellular processes, including proliferation, migration, and apoptosis, and the dysregulation of these signaling networks favors the growth and persistence of

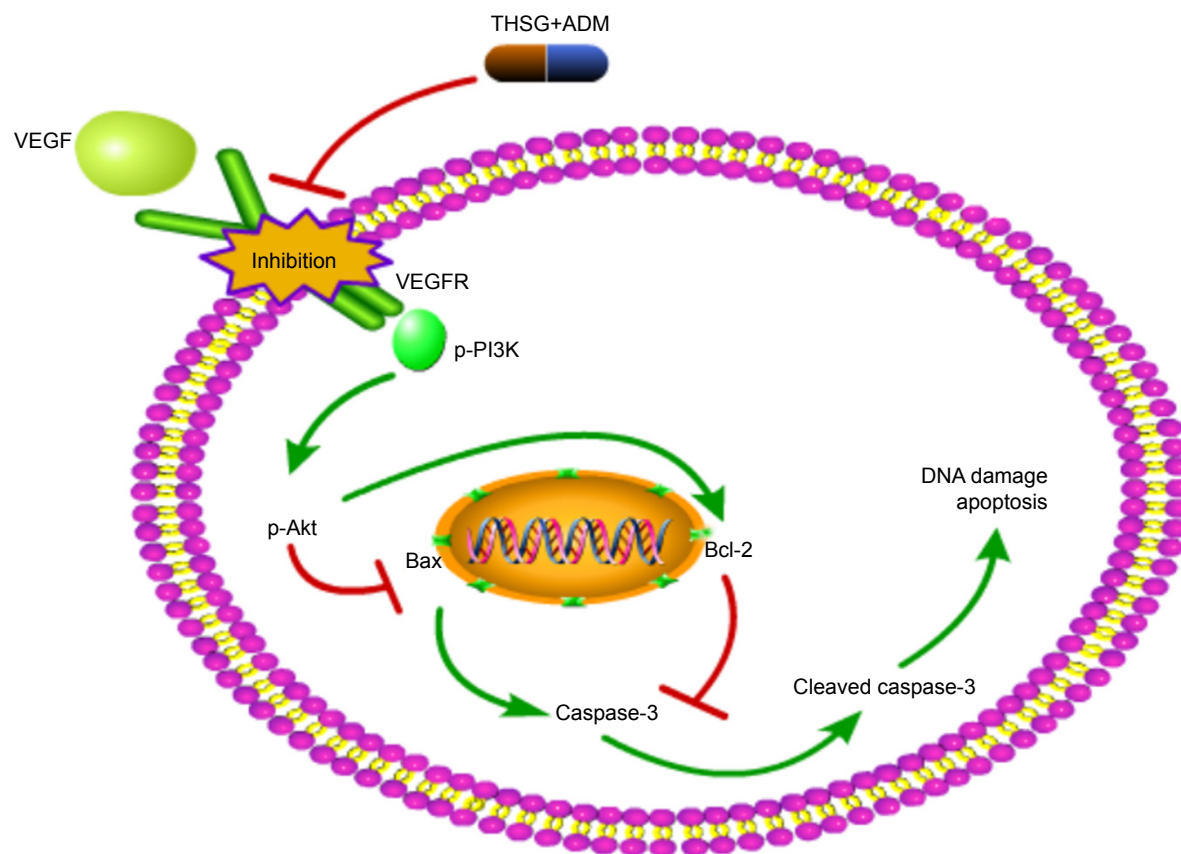


Figure 6 The proposed signal pathway with THSG and ADM in MCF-7 cells.
Abbreviations: ADM, Adriamycin; THSG, 2,3,5,4'-Tetrahydroxystilbene-2-O- β -D-glucoside.

human cancer.³² A flow cytometry assay demonstrated that the THSG proportion increased the cell population in early apoptosis in Q4, ADM, and the combination of both, which primarily distributed the cell population into late apoptosis in Q2, which was similar to the report that attributed this effect to the similarities in the excitation wavelength between PI and ADM autofluorescence.³³ This study further identifies the mechanism of the aforementioned apoptosis. Bax and cleaved caspase-3 are proapoptotic proteins that were upregulated and antiapoptotic Bcl-2 was downregulated, suggesting activation of the apoptotic pathway.^{34,35} Resveratrol has been used in breast cancer chemoprevention, and the molecular mechanism of this effect is the induction of apoptosis in cell and animal models of breast cancer.³⁶ THSG, a resveratrol analog, for the first time demonstrated regulation of apoptosis-related proteins and promotion of breast cancer cell apoptosis in vitro. Additionally, the two drug combination synergized to regulate apoptosis-related proteins.

Akt kinase is phosphorylated by PI3K and controls cell apoptosis by regulating the antiapoptotic Bcl-2 protein.³² Thus, we concluded that THSG and ADM individually may exert antitumor cellular proliferation effects via the inhibition

of the VEGF/PI3K/Akt pathway and then induce apoptosis by affecting apoptosis-related proteins, as the two pathways are integrated. In addition, the combination treatment exhibited synergism in a similar manner (Figure 6). Importantly, THSG is water soluble and exerts almost no cardiac toxicity. Accordingly, THSG, as an adjuvant agent, served as a drug that can regulate the VEGF/PI3K/Akt pathway for treating breast cancer, which could minimize the adverse effects of ADM, improve clinical outcomes, and contribute to elevating the quality of life of patients.

Acknowledgment

This research was funded by the National Natural Science Foundation of China (No. 81603110), and the Science and Technology Project of Jiaxing City (No. 2016BY28009).

Disclosure

The authors report no conflicts of interest in this work.

References

- McGuire A, Brown JA, Kerin MJ. Metastatic breast cancer: the potential of miRNA for diagnosis and treatment monitoring. *Cancer Metastasis Rev.* 2015;34(1):145–155.

2. Viedma-Rodríguez R, Baiza-Gutman L, Salamanca-Gómez F, et al. Mechanisms associated with resistance to tamoxifen in estrogen receptor-positive breast cancer (review). *Oncol Rep*. 2014;32(1):3–15.
3. Shenkenberg TD, Von Hoff DD. Mitoxantrone: a new anticancer drug with significant clinical activity. *Ann Intern Med*. 1986;105(1):67–81.
4. Menna P, Recalcati S, Cairo G, Minotti G. An introduction to the metabolic determinants of anthracycline cardiotoxicity. *Cardiovasc Toxicol*. 2007;7(2):80–85.
5. Thorn CF, Oshiro C, Marsh S, et al. Doxorubicin pathways: pharmacodynamics and adverse effects. *Pharmacogenet Genomics*. 2011;21(7):440–446.
6. Hanušová V, Boušová I, Skálová L. Possibilities to increase the effectiveness of doxorubicin in cancer cells killing. *Drug Metab Rev*. 2011; 43(4):540–557.
7. Chimento A, Sirianni R, Saturnino C, Caruso A, Sinicropi MS, Pezzi V. Resveratrol and its analogs as antitumoral agents for breast cancer treatment. *Mini Rev Med Chem*. 2016;16(9):699–709.
8. Lin CL, Hsieh SL, Leung W, et al. 2,3,5,4'-tetrahydroxystilbene-2-O-β-D-glucoside suppresses human colorectal cancer cell metastasis through inhibiting NF-κB activation. *Int J Oncol*. 2016;49(2):629–638.
9. Xu M, Wang C, Zhu M, Wang X, Zhang L, Zhao J. 2,3,5,4'-tetrahydroxy diphenylethylene-2-O-glucoside inhibits the adhesion and invasion of A549 human lung cancer cells. *Mol Med Rep*. 2017;16(6): 8900–8906.
10. Kimura Y, Okuda H. Effects of naturally occurring stilbene glucosides from medicinal plants and wine, on tumour growth and lung metastasis in Lewis lung carcinoma-bearing mice. *J Pharm Pharmacol*. 2000; 52(10):1287–1295.
11. Yang PY, Almofti MR, Lu L, et al. Reduction of atherosclerosis in cholesterol-fed rabbits and decrease of expressions of intracellular adhesion molecule-1 and vascular endothelial growth factor in foam cells by a water-soluble fraction of *Polygonum multiflorum*. *J Pharmacol Sci*. 2005;99(3):294–300.
12. Zhang SH, Wang WQ, Wang JL. Protective effect of tetrahydroxystilbene glucoside on cardiotoxicity induced by doxorubicin in vitro and in vivo. *Acta Pharmacol Sin*. 2009;30(11):1479–1487.
13. Lin EY, Bayarsengee U, Wang CC, Chiang YH, Cheng CW. The natural compound 2,3,5,4'-tetrahydroxystilbene-2-O-β-D-glucoside protects against adriamycin-induced nephropathy through activating the Nrf2-Keap1 antioxidant pathway. *Environ Toxicol*. 2018;33(1):72–82.
14. Chou TC. Theoretical basis, experimental design, and computerized simulation of synergism and antagonism in drug combination studies. *Pharmacol Rev*. 2006;58(3):621–681.
15. Chou TC, Talalay P. Quantitative analysis of dose-effect relationships: the combined effects of multiple drugs or enzyme inhibitors. *Adv Enzyme Regul*. 1984;22:27–55.
16. Zhang N, Fu JN, Chou TC. Synergistic combination of microtubule targeting anticancer fludelon with cytoprotective panaxytriol derived from panax ginseng against MX-1 cells in vitro: experimental design and data analysis using the combination index method. *Am J Cancer Res*. 2016;6(1):97–104.
17. Chen Y, Wang L, Pitzer AL, Li X, Li PL, Zhang Y. Contribution of redox-dependent activation of endothelial Nlrp3 inflammasomes to hyperglycemia-induced endothelial dysfunction. *J Mol Med*. 2016; 94(12):1335–1347.
18. Jiang Z, Xu J, Long M, Tu Z, Yang G, He G. 2, 3, 5, 4'-tetrahydroxystilbene-2-O-beta-D-glucoside (THSG) induces melanogenesis in B16 cells by MAP kinase activation and tyrosinase upregulation. *Life Sci*. 2009;85(9–10):345–350.
19. Gao S, Liu Z, Li H, Little PJ, Liu P, Xu S. Cardiovascular actions and therapeutic potential of tanshinone IIA. *Atherosclerosis*. 2012;220(1):3–10.
20. Qureshi R, Yildirim O, Gasser A, et al. FL3, a synthetic flavagline and ligand of prohibitins, protects cardiomyocytes via STAT3 from doxorubicin toxicity. *PLoS One*. 2015;10(11):e0141826.
21. Gu J, Hu W, Song ZP, Chen YG, Zhang DD, Wang CQ. Resveratrol-induced autophagy promotes survival and attenuates doxorubicin-induced cardiotoxicity. *Int Immunopharmacol*. 2016;32:1–7.
22. Kim TH, Shin YJ, Won AJ, et al. Resveratrol enhances chemosensitivity of doxorubicin in multidrug-resistant human breast cancer cells via increased cellular influx of doxorubicin. *Biochim Biophys Acta*. 2014; 1840(1):615–625.
23. Huang F, Wu XN, Chen J, Wang WX, Lu ZF. Resveratrol reverses multidrug resistance in human breast cancer doxorubicin-resistant cells. *Exp Ther Med*. 2014;7(6):1611–1616.
24. Sheu MT, Jhan HJ, Hsieh CM, Wang CJ, Ho HO. Efficacy of antioxidants as a Complementary and Alternative Medicine (CAM) in combination with the chemotherapeutic agent doxorubicin. *Integr Cancer Ther*. 2015;14(2):184–195.
25. Zhang L, Rui YC, Qiu Y, Li TJ, Liu HJ, Chen WS. [Expression of VEGF in endothelial cells and the effects of 2, 3, 5, 4'-tetrahydroxystilbene-2-O-beta-D-glucoside]. Japanese [with English abstract]. *Yao Xue Xue Bao*. 2004;39(6):406–409.
26. Mu Y, Xu Z, Zhou X, et al. 2,3,5,4'-Tetrahydroxystilbene-2-O-β-D-Glucoside attenuates ischemia/reperfusion-induced brain injury in rats by promoting angiogenesis. *Planta Med*. 2017;83(8):676–683.
27. de la Vega M, Díaz-Cantón E, Alvarez RH. Novel targeted agents for the treatment of advanced breast cancer. *Future Med Chem*. 2012; 4(7):893–914.
28. Mayer IA, Arteaga CL. The PI3K/AKT pathway as a target for cancer treatment. *Annu Rev Med*. 2016;67:11–28.
29. Thorpe LM, Yuzugullu H, Zhao JJ. PI3K in cancer: divergent roles of isoforms, modes of activation and therapeutic targeting. *Nat Rev Cancer*. 2015;15(1):7–24.
30. Lee JJ, Loh K, Yap YS. PI3K/Akt/mTOR inhibitors in breast cancer. *Cancer Biol Med*. 2015;12(4):342–354.
31. Ola R, Dubrac A, Han J, et al. PI3 kinase inhibition improves vascular malformations in mouse models of hereditary haemorrhagic telangiectasia. *Nat Commun*. 2016;7:13650.
32. Narla G, Sangodkar J, Ryder CB. The impact of phosphatases on proliferative and survival signaling in cancer. *Cell Mol Life Sci*. 2018; 75(15):2695–2718.
33. Xie J, Liu JH, Liu H, et al. Tanshinone IIA combined with Adriamycin inhibited malignant biological behaviors of NSCLC A549 cell line in synergistic way. *BMC Cancer*. 2016;16(1):899.
34. Green DR, Reed JC. Mitochondria and apoptosis. *Science*. 1998; 281(5381):1309–1312.
35. Rossé T, Olivier R, Monney L, et al. Bcl-2 prolongs cell survival after Bax-induced release of cytochrome c. *Nature*. 1998;391(6666): 496–499.
36. Sinha D, Sarkar N, Biswas J, Bishayee A. Resveratrol for breast cancer prevention and therapy: preclinical evidence and molecular mechanisms. *Semin Cancer Biol*. 2016;40–41:209–232.

Drug Design, Development and Therapy

Dovepress

Publish your work in this journal

Drug Design, Development and Therapy is an international, peer-reviewed open-access journal that spans the spectrum of drug design and development through to clinical applications. Clinical outcomes, patient safety, and programs for the development and effective, safe, and sustained use of medicines are the features of the journal, which

has also been accepted for indexing on PubMed Central. The manuscript management system is completely online and includes a very quick and fair peer-review system, which is all easy to use. Visit <http://www.dovepress.com/testimonials.php> to read real quotes from published authors.

Submit your manuscript here: <http://www.dovepress.com/drug-design-development-and-therapy-journal>